

Supplementary information

Determination of Young's modulus

a) Cylindrical Punch Indentation Experiment

The purpose of this brief note is to put down the relations needed to extract Young's modulus from a compliance measurement made by indenting a sample using a rigid cylindrical punch.

In the schematic figure S1, a circular cylindrical punch with radius a indents an elastic foundation that is very large in the plane of the contact, i.e., $L \gg a$. However, its thickness, h , may or may not be large compared to a .

In the limit when $h \gg a$, we have indentation by a rigid circular punch of an elastic half space. In this case^{16,24},

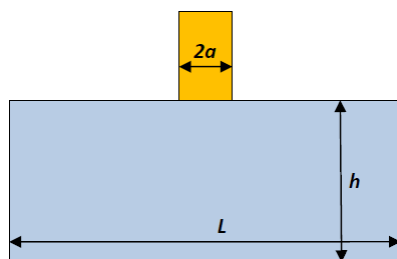


Figure S1: Schematic of flat cylindrical punch with diameter $2a$ used to indent a gel block of height h and diameter L

$$\lim_{h/a \rightarrow \infty} \left(\frac{d\delta}{dP} \right) = C_{\infty} = \frac{1}{2E^*a} \quad [s1]$$

where δ is the displacement of the indenter, P is the measured load, C_{∞} is the compliance in the limit $h \gg a$ or $h/a \rightarrow \infty$, $E^* = E/(1-\nu^2)$ is the plane strain Young's modulus, and ν is Poisson's ratio. If the material is incompressible, then $\nu = 1/2$, and equation s1 becomes

$$\lim_{h/a \rightarrow \infty} \left(\frac{d\delta}{dP} \right) = C_{\infty} = \frac{1}{2E^*a} = \frac{1-\nu^2}{2Ea} = \frac{3}{8Ea} = \frac{1}{8Ga} \quad [s2]$$

where we have used the relation $G = E/(2(1+\nu))$. This is the same result as given in Long *et al.*¹⁶ (equations 24 a, b) who have additionally shown that for finite h , the compliance C can be written in terms of C_{∞} in the following way:

$$\frac{d\delta}{dP} = C = C_{\infty} \left(\frac{1}{1+\chi(\eta)} \right); \eta = \frac{a}{h} \quad [s3]$$

$$\chi(\eta) = \frac{1.095\eta + 1.3271\eta^2 + 0.1431\eta^4}{0.9717}$$

So, since C is the measured quantity, our expression for Young's modulus is

$$E^* = \frac{1}{2aC} \left(\frac{1}{1+\chi(\eta)} \right); \eta = \frac{a}{h} \quad [s4]$$

$$\chi(\eta) = \frac{1.095\eta + 1.3271\eta^2 + 0.1431\eta^4}{0.9717}$$

A typical load-displacement plot is shown in figure S2

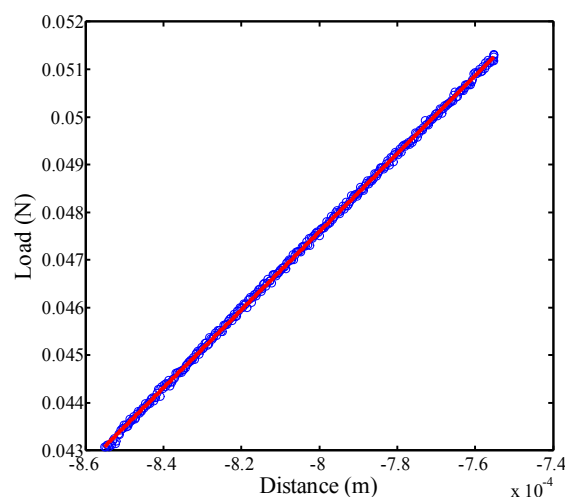


Figure S2: Load measured as a function of indentation depth (Distance) in a typical contact compliance test. The compliance C is the inverse of the slope.

a) Beam bending

The modulus was measured using the linear elastic moment-curvature relationship of beam theory

$$M = EIk \quad [s5]$$

where M is the moment on the beam fixed at one end, I is the moment of inertia of the rectangular cross-section of the beam and k is the curvature of the bent element.

Equation (s5) can be re-written in terms of the distance s along the neutral axis of the beam

$$\frac{M(s)}{EI} = \frac{d\theta}{ds} \quad [s6]$$

Integrating eq. s6

$$\int M(s)ds = EI \int d\theta \quad [s7]$$

That is, the integral of the moment is linearly related to change in angle, and the slope is EI . The integral of the moment is plotted

as a function of the angle and from the slope the modulus is obtained (figure S3).

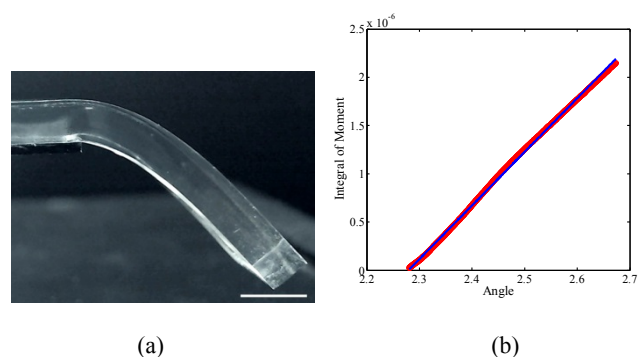


Figure S3: (a) Picture of a gel beam fixed at one end and freely hanging on the other (scale bar ~ 1 cm). The profile of the beam is read using MATLAB code for determination of the curvature.

Confirmation that the gel fills the patterned PDMS

We re-confirmed the assumption that the liquid gel wets the PDMS master completely. A section of the PDMS master was cut and laid flush on the bottom of the petri-dish such that the ridges were orientated perpendicular to it. After filling and gelation images were taken through the transparent base of the petri-dish. Figure S4 shows the optical micrographs of gel filled PDMS master, demonstrating that the gel does intrude completely into the PDMS.

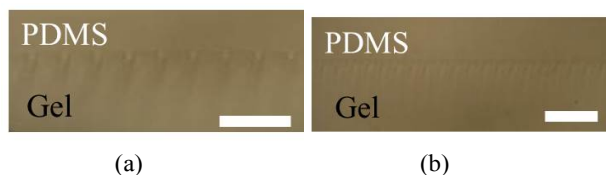


Figure S4: Optical micrographs (scale bar 100 μm) of gel ($E \sim 23$ kPa)-filled PDMS master for periodic ridge geometry (a) $h \sim 13$ μm , $\lambda \sim 35$ μm and (b) $h \sim 2.7$ μm , $\lambda \sim 25$ μm .

Height reduction of high ridge geometry

In the experimental results part of the main text we presented the variation of the ratio of deformed to initial height for the high ridge geometry. Figure S5 shows the absolute heights of the PDMS and the deformed gel samples for the ridge geometry with $h \sim 13$ μm . A lower deformed height (h_d) was measured for a gel with lower modulus (E).

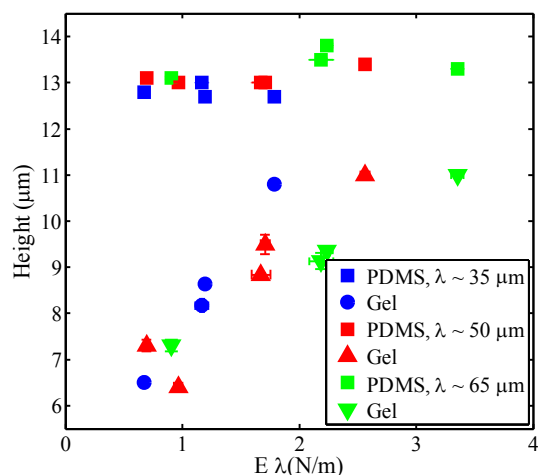


Figure S5: Measured initial height of PDMS ridge/channel samples ($h \sim 13$ μm , square symbols) and the corresponding gel height (h_d) for three different periodic spacing λ (symbols circles, triangles and inverted triangles represent, respectively, spacing of $\lambda \sim 35$, 50 and 65 μm (see Table 1) and five different moduli (E).

FEM analysis for low height ridge geometry ($h \sim 2.7$ μm)

To test the validity of the small strain theory, we applied also applied the FEM analysis to the case of shallow ridges for which small strain theory satisfactorily predicted the full deformed profile of the gel after demolding. Figure S6 shows that the least square fitting results of FEM analysis to experimental data yield a surface tension σ of 105.0 ± 17.6 mN/m which is consistent with that obtained from the small strain theory ($\sigma = 100.0 \pm 9.4$ mN/m).

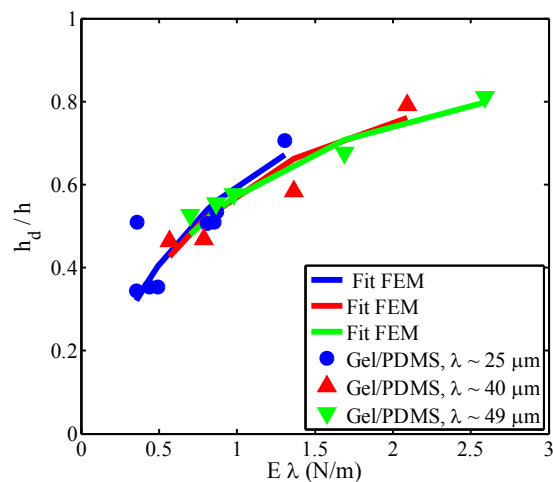


Figure S6: Measured reduction in gel height (ratio of final to initial height h/h_0) and FEM analysis based least square fits (continuous lines) for the height reduction as a function of varying elastic moduli E and three different periods λ (symbols circles, triangles and inverted triangles represent, respectively, spacing of $\lambda \sim 25$, 40 and 49 μm)

FEM analysis: Validity of Neo-Hookean model

We applied an alternate model to the Neo-Hookean to ascertain its validity. The linear elastic model was used to estimate the deformed heights (figure S6). We observe that for the surface tension of approximately 110 mN/m, which is close to estimated surface stress for low strain case, the two models deviate by less than 8% (figure S7).

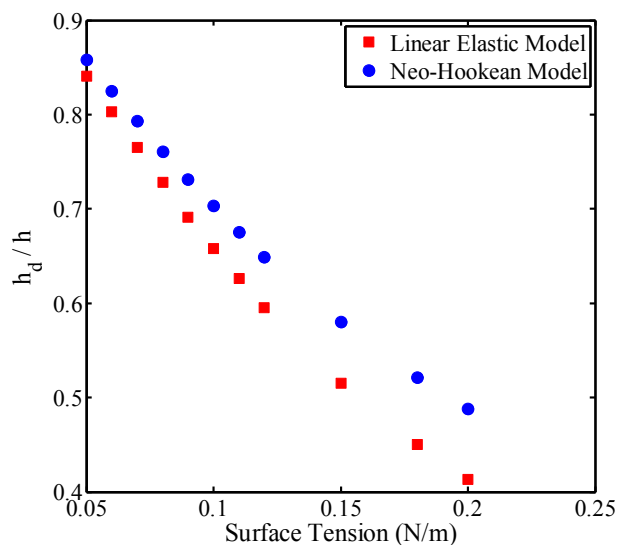


Figure S7: Comparison of deformed heights (normalized by initial height) for a given surface tension for the neo-Hookean versus linear elastic material models.